

Fig. 21. The porosity variation (comes from simulated results) over reduction time during HyDR for different pellet size (a) 950 °C (b) 1000 °C.

reduction, resulting in lower porosity. In contrast, larger pellets with less curvature are more prone to uneven stress distribution, which can lead to increased porosity and a higher probability of cracking. This effect, combined with the inherent differences in geometry and curvature of pellets of different sizes, contributes to the observed differences in density and porosity distribution, with larger pellets being more prone to the formation of internal voids and less dense regions. Therefore, it can be concluded that the curvature effect together with the improved thermal conditions may favor a more uniform reduction in pellet volume. In addition, the overall rates of porosity development also reflect the combined effects of temperature and curvature, with the greatest overall change observed for big pellets at 1000 °C (24.89). This could be due to the larger pellets being better able to maintain a higher porosity throughout the reduction process when exposed to higher temperatures, despite their lower surface area to volume ratio.

From a kinetic point of view, the higher rate indicates that the entropy generated by chemical reactions is greater at 1000 °C because the reactions take place faster [10]. In addition, higher temperatures and larger pellets can be shown to have higher rates, indicating an increase in porosity. This increase in porosity can lead to a decrease in entropy generation as gas penetration is improved and flow resistance is reduced [1,55]. The higher porosity evolution rates at higher temperatures and in larger pellets cause an increase in pore complexity and tortuosity (see Table 15). The interplay between pore structure and gas flow dynamics, especially diffusion and convection in porous media, plays a crucial role in the HyDR process of iron oxide pellets [59]. Table 6 shows that the porosity evolution rate varies significantly with pellet size and temperature, which in turn influences the gas transport mechanisms. Figs. 22 and 21 also illustrate that with increasing porosity, especially at higher temperatures, there is a greater free volume for gas flow, which promotes both diffusion and convection within the pellets. The observed trend shows that larger pellets and higher temperatures lead to greater porosity variation, which can result in more pronounced convective behavior. This is likely due to the larger pathways available for gas movement and the thermal expansion of gasses at higher temperatures. Consequently, this affects the reduction kinetics, with larger pellets exhibiting a faster increase in porosity at 1000 °C and a steeper decline after the peak, suggesting changes in the dominant gas flow mechanism as the reduction progresses. In addition, the curvature of the pellets has a significant effect on the surface area available for gas-solid interactions. Smaller pellets with higher curvature have a greater surface area to volume ratio, which improves contact between the reducing gas and the

iron oxide surface. This larger contact area allows for more uniform and efficient reduction throughout the pellet. Conversely, larger pellets with less curvature have a smaller surface area in relation to their volume, which can lead to less uniform reduction. The reason for this is a more pronounced concentration gradient of the reducing gas in the pellet, which can lead to uneven reduction and localized zones with higher porosity. In addition, the shape of the pellet influences the path and flow rate of the gasses in the void spaces, which affects the overall reduction kinetics.

The increased tortuosity can act as an obstacle to gas flow, and reduce diffusion and the reduction effect, prolonging the time to reduction [10]. The high porosity rates for large pellets at 1000 °C imply that the tortuosity is also likely to be higher, which can lead to increased entropy generation. Entropy generation increases with the decrease in porosity and gas fraction due to the reduced exchange surfaces [1,2]. This is because the lower porosity rates for small pellets at 950 °C compared to larger pellets at 1000 °C, where the reduced exchange surfaces could lead to increased entropy generation. This more likely has a significant effect on the $W \rightarrow Fe$ transition as a sluggish step. The data given in Table 5 show that the reduction rate for the $W \rightarrow Fe$ transition increases significantly for all pellet sizes at 1000 °C compared to 950 °C. This increase in rate could reduce the entropy generation by chemical reactions as the reactions occur faster, despite the increased tortuosity. It can be concluded that at higher temperatures, the increased reduction rates and porosity evolution rates lead to higher entropy generation due to chemical reactions but possibly lower entropy generation due to mass transfer as gas penetration improves. However, the increased tortuosity at higher temperatures and in larger pellets may increase entropy generation due to the additional resistance to gas flow. The total energy input to the reduction process is a balance between these factors and would be higher for processes that generate more entropy, especially in the initial stages of reduction where both the chemical reaction and gas diffusion are rate-limiting steps. As the process progresses, the thermal gradient and the driving force for the chemical reactions reduce, leading to a decrease in entropy generation.

The reduction process carried out at 950 °C for 90 min leads to an increase in free volume of approx. 3.5%, while at 1000 °C the free volume increases by a smaller margin of 0.26%. At the same time, a decrease in the average pore diameter can be observed at both temperatures. This indicates that the microstructural transformation of the pellets during reduction is not only a product of their initial porosity, but is also characterized by an increase in free volume and the introduction

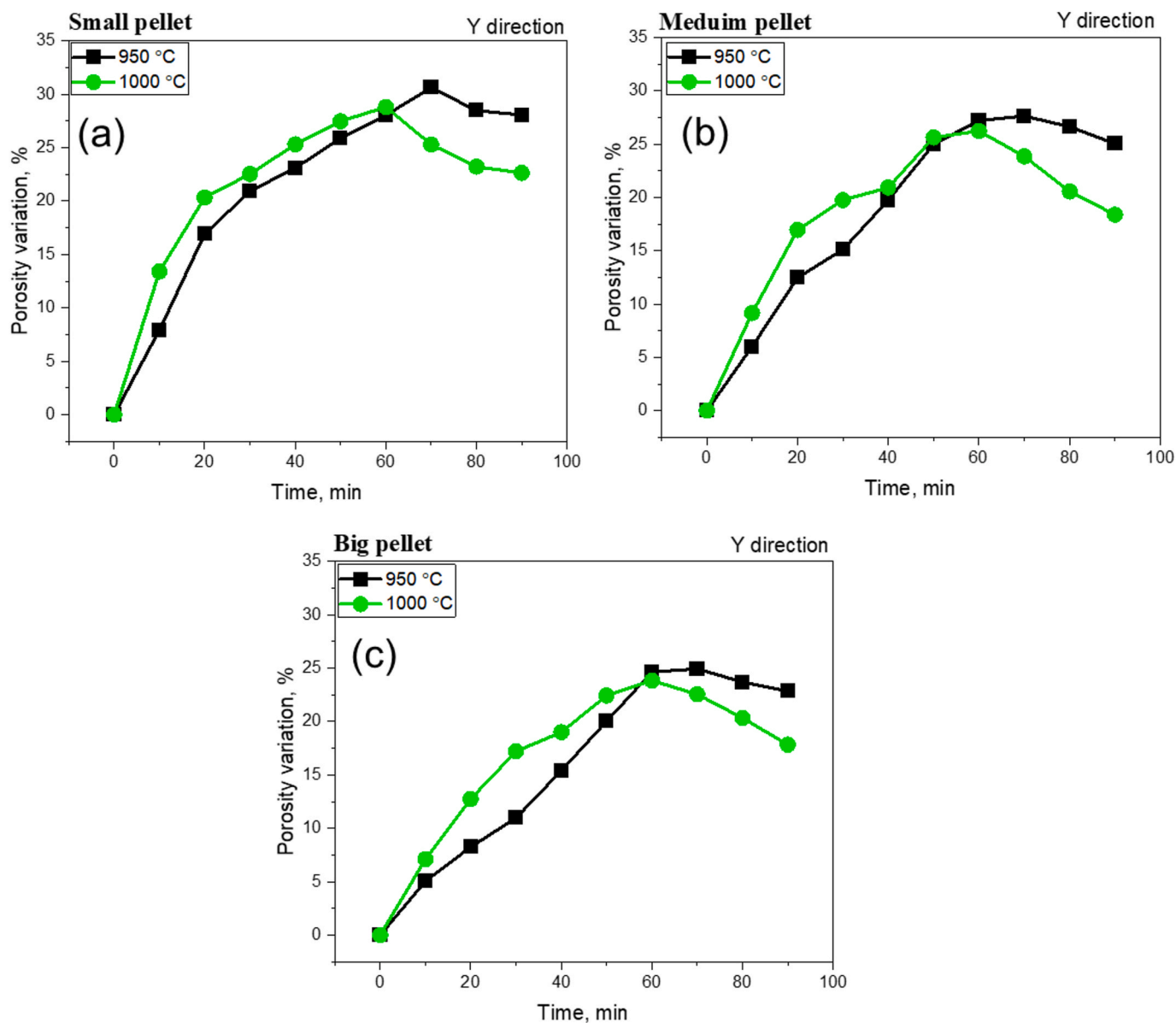


Fig. 22. Comparison between the porosity variation (comes from simulated result) over reduction time at two temperatures of 950 °C and 1000 °C in Y direction for different pellet size (a) small, (b) medium, and (c) big.

of various lattice defects, such as dislocations and cracks. This conclusion is in line of results reported by Kim et al. [1,40]. These changes are an indication of the volume mismatch and the resulting tensions that arise between the reactant and the product phase during the reduction process. This is illustrated by the increased porosity and cracking seen in the accompanying figures, which show the HyDR process at different temperatures and pellet sizes. Obviously, the transformation of $W \rightarrow Fe$ is accompanied by significant changes in the microstructure of the pellet. In particular, the elastic work required to compensate for the volume changes during the nucleation of Fe acts as an obstacle [1,56], as indicated by the increase in the reduction rate for the $W \rightarrow Fe$ reaction at the higher temperature of 1000 °C. This increased rate indicates that at this temperature a faster phase transition and consequently a larger volume change takes place, which cannot be completely overcome by elastic deformation of the microstructure of the pellet. When the Fe core forms, the significant volume change associated with this reaction stage and the associated deformation exceed the limits of what can be handled by elastic deformation. In addition, the increase in porosity and cracking as a result of reduction, which is particularly evident in smaller pellets at

higher temperatures (1000 °C), leads to a significant reduction in compressive strength as the initial conversion of H to M weakens the structural integrity of the pellet. This is also influenced by pellet size, with larger pellets exhibiting higher strength due to slower reduction kinetics and less pronounced porosity changes [60,61]. The data showing an increased porosity rate, particularly at 1000 °C, is consistent with the concept that the resulting mechanical stresses lead to the formation of cracks as well as creep voids and dislocations within the pellet. These microstructural defects are an expression of the material's attempt to relieve stresses, indicating that the reduction process causes not only chemical changes but also significant mechanical changes.

From a thermodynamic point of view, it should be noted that temperature plays an important role in influencing the reaction pathways and the establishment of equilibrium states during the direct reduction of iron oxide pellets. In the context of iron oxide reduction using pure hydrogen, temperature exerts a decisive influence on the reaction pathways and the equilibrium states, as shown in Table 6. The thermodynamic feasibility of these reactions is determined by the change in Gibbs free energy (ΔG), which is a function of enthalpy change (ΔH),

absolute temperature (T) and entropy change (ΔS), according to the equation $\Delta G = \Delta H - T\Delta S$. The reduction reactions proceed via intermediate steps with the ultimate goal of converting iron oxides into elemental iron. For clarification, here are the most important intermediate and total reduction reactions together with their standard changes in Gibbs free energy at 1000 K,

Intermediate reduction reactions [62–65].

(1) $\text{Fe}_2\text{O}_3 + 3\text{H}_2 \rightarrow 2\text{Fe} + 3\text{H}_2\text{O}$	$\Delta G^\circ_1 \cong -99 \text{ kJ/mol}$	(at 1000 K)
(2) $\text{Fe}_3\text{O}_4 + 4\text{H}_2 \rightarrow 3\text{Fe} + 4\text{H}_2\text{O}$	$\Delta G^\circ_2 \cong -115 \text{ kJ/mol}$	(at 1000 K)
(3) $\text{FeO} + \text{H}_2 \rightarrow \text{Fe} + \text{H}_2\text{O}$	$\Delta G^\circ_3 \cong -65 \text{ kJ/mol}$	(at 1000 K)

Total reduction reaction [64–66].

$\text{Fe}_2\text{O}_3 + 3\text{H}_2 \rightarrow 2\text{Fe} + 3\text{H}_2\text{O}$	$\Delta G^\circ_{\text{total}} \cong -26.2 \text{ kJ/mol}$	(at 1000 K)
--	--	-------------

As the temperature increases, the $T\Delta S$ term becomes larger, which leads to a more negative ΔG and thus promotes the spontaneous progression of the reduction reactions. Furthermore, it can be deduced that W is thermodynamically more stable compared to H and M at 1000 °C and hydrogen as reducing agent, which is indicated by the relatively less negative ΔG° value for the W reduction reaction. In fact, the higher stability of W at 1000 °C indicates that under a range of conditions where the system does not achieve complete reduction, W is still remained in Fe matrix. This incomplete reduction can lead to a heterogeneous microstructure within the pellet, where regions of unreduced W coexist with reduced iron. This heterogeneity can contribute to an increase in porosity and tortuosity, as can be seen in the previous figures, as the formation of W involves a reduction in volume compared to H and M, creating voids within the pellet matrix. In addition, the presence of different phases with different volumes and thermal expansion coefficients can lead to internal stresses during cooling, potentially causing cracks and further compromising the mechanical integrity of the pellets. The thermodynamic analysis supports our experimental observations and numerical calculations that higher temperatures lead to accelerated reduction kinetics and significant microstructural changes, such as increased porosity. In addition, the bigger pellet size can be expected to contribute to a specific phase composition and different reduction behavior compared to the smaller pellet. The presence and distribution of elements such as silicon, aluminum and calcium in the larger pellet can affect the reaction kinetics and the overall mechanical properties of the pellet.

The initial inhomogeneity seen in the simulated results is consistent with the early stage of porosity development, where porosity increases rapidly, as shown in previous figures. In addition, the observed porosity changes at 950 °C are consistent with the reported slower increase in porosity compared to the faster porosity evolution at 1000 °C. The images document the slower kinetics at the lower temperature, which could lead to a more uniform porosity distribution over time. In the middle stages, the contour patterns indicate enhanced gas transport within the pellet, supporting the notion that increased porosity improves gas-solid interactions. In the later stages, the images show that although porosity increases, the distribution becomes more uneven, indicating potential limitations in the reduction process such as the integrity of the pellet and the onset of sintering. This is important for optimizing the HyDR process to achieve a balance between achieving sufficient porosity for effective reduction and maintaining pellet strength. At a temperature of 1000 °C, the reduction kinetics are primarily driven by temperature, while porosity has a secondary effect. The experimental and simulated results show that the reduction rate and porosity evolution rate are generally higher at 1000 °C than at 950 °C, confirming that higher temperatures enhance the reduction process. This is consistent with the observation that the degree of reduction at the higher temperature of 1000 °C is more influenced by porosity due to the larger surface area and gas-solid interactions associated with higher porosity. Based on the microtomography and the simulated images we provided you with

earlier, we were able to determine that the porosity within the pellets is unevenly distributed, which would lead to fluctuations in gas velocity similar to those described above [29].

The presence of larger pores and a complex pore network, as suggested by the higher porosity values in the tables, would create regions of lower resistance where the gas velocity increases. The results also show that the complex pore structure leads to increased flow resistance when gas enters the pores, which is particularly relevant for tortuosity [14,15]. The larger pellets, especially at 1000 °C, exhibit higher porosity evolution rates, indicating an increase in pore complexity and tortuosity. This increased tortuosity acts as a barrier to gas flow, making it more difficult for the gas to penetrate the interior of the pellet and potentially slowing the rate of reduction in the later stages, where tortuosity would have the greatest impact. Finally, the gas velocity in the pores is anisotropic and is influenced by several factors, including pore size and shape [29,39]. At 1000 °C, the porosity rate is significantly increased for all pellet sizes, confirming the assumption that higher temperatures promote faster and more extensive microstructural changes, including greater porosity and lower resistance to gas flow. These changes improve gas-solid interaction due to the greater number of reactive sites and improve the efficiency of the reduction process. The anisotropic gas velocity within the pores [29], which is influenced by the pore size and shape, is also obvious. When the evolution of porosity reaches its peak, we can conclude that the gas velocity increases accordingly in regions of lower resistance, especially near the pellet surface or where larger pores are present. This phenomenon highlights the importance of controlling pellet microstructure and temperature to optimize the direct reduction process, as porosity plays a critical role in facilitating effective gas transport and reaction kinetics. Therefore, the porosity evolution rate is higher at larger pellet sizes and higher temperatures, which means that the gas velocity is higher near the pellet surface and in larger pores. This is consistent with the idea that gas flow favors regions with larger pores and lower resistance, which would also correlate with the SEM images showing larger, more interconnected pores in pellets exposed to higher temperatures.

The present study underlines the need to optimize the direct reduction process in order to improve industrial efficiency and product quality. Based on the experimental and numerical results, a multi-faceted approach to optimization is recommended: (1) Careful control of the reduction temperature to balance the kinetics of the reduction with the mechanical stability of the iron pellets, as higher temperatures accelerate the reduction but may compromise the structural integrity due to increased porosity and cracking. (2) Adjusting the size of the iron oxide pellets to control heat transfer and gas diffusion rates, optimize reduction uniformity and minimize thermal stresses. (3) The use of staged reduction strategies, where reduction conditions are adjusted at different stages to favor the formation of specific iron oxide phases, can result in a better controlled microstructure. (4) Continuous monitoring and adjustment of hydrogen flow rates to ensure that the reducing environment is efficiently maintained throughout the process.

Furthermore, the relatively high reaction rates observed with larger iron oxide pellets have significant practical implications for industrial direct reduction processes. Larger pellets, due to their greater porosity and higher reaction rates, are particularly well suited to processes where rapid reduction is the primary concern and where the mechanical integrity of the pellets after reduction is less important. For example, in processes using a multi-stage reduction furnace, larger pellets can be advantageous as they enable faster throughput and greater efficiency in the initial stages of reduction. Furthermore, in processes that involve size reduction after reduction, the fragility caused by the higher porosity of larger pellets can actually be an advantage as it reduces the energy required for subsequent size reduction. However, in processes that require high-strength pellets, such as in a shaft furnace where the pellets are subjected to significant mechanical stress, the size of the pellets must be carefully controlled to prevent structural failure. Therefore, understanding the relationship between particle size and reaction kinetics is